AGU PUBLICATIONS

Geophysical Research Letters

RESEARCH LETTER

10.1002/2014GL061802

Key Points:

- The XBT biases account for 3 to 8% error in MOC and MHT
- Impact of XBT biases are small relative to MOC natural variability
- Historical biases produce a positive trend on MOC/MHT estimates after the 1990s

Supporting Information:

- Text S1 and Figure S1

Correspondence to:
M. Goes,
marlos.goes@noaa.gov

Citation:
Goes, M., M. Baringer, and G. Goni (2015), The impact of historical biases on the XBT-derived meridional overturning circulation estimates at 34°S, *Geophys. Res. Lett.*, *42*, doi:10.1002/2014GL061802.

Received 12 SEP 2014
Accepted 27 JAN 2015
Accepted article online 29 JAN 2015

The impact of historical biases on the XBT-derived meridional overturning circulation estimates at 34°S

Marlos Goes[1,2], Molly Baringer[1], and Gustavo Goni[1]

[1]NOAA/AOML, Miami, Florida, USA, [2]CIMAS, University of Miami, Miami, Florida, USA

Abstract An observational system based on high-density expendable bathythermograph (XBT) data has provided the longest record of the South Atlantic meridional overturning and heat transport estimates across 34°S. Measurement biases are a point of concern for the capability of an XBT system to capture long-term trends in volume and heat transports, and the impact of such biases on the meridional overturning estimates has never been quantified. In the present study, the sensitivity of the meridional overturning circulation and heat transport to uncertainties in XBT measurements is quantified under the framework of an eddy-resolving model simulation. Results show that XBT measurement biases after 2010 can translate into small meridional overturning errors on the order of 3% or 0.38 Sv ($1 \text{Sv} = 10^6 \text{ m}^3 \text{ s}^{-1}$), and 0.025 PW ($1 \text{ PW} = 10^{15}$ W) or 8% of the meridional heat transport in the model. Historical XBT-derived trends in transport estimates across 34°S are stronger and statistically significant after the late 1990s, 0.3 Sv decade^{-1} and 0.02 PW decade^{-1}. These trends are mostly due to the XBT linear depth bias, with smaller contributions associated with temperature and depth offsets from the historical record. Long-term trends calculated from Simple Ocean Data Assimilation reanalysis, estimated as 0.1 Sv/decade and 0.006 PW/decade, are 3 times smaller than the XBT-derived historical trends. Therefore, an adequate correction of historical XBT data is necessary for an early detection of trends in the meridional overturning circulation and heat transport.

1. Introduction

Historically, expendable bathythermographs (XBTs) were designed for Navy applications that required a cost effective, flexible, and fast means of determining the local temperature profile and the sound speed channel in the upper ocean. The ease of deployment and low cost comes at the expense of its measurement accuracy. XBT data have larger errors than the ones produced by conductivity-temperature-depth (CTD) stations, partly because XBT probes do not measure depth. Instead, they rely on a fall rate equation (FRE) that relates the time of descent with depth. FRE errors, stated by the manufacturer as ±5 m or 2% of depth, whichever is greater, generate the largest uncertainty in XBT temperature measurements. In addition, temperature accuracy from XBT thermistors suffers from the influence of several factors, such as wire resistance imbalance, time response to thermal gradients, and static bath calibrations (see *Reseghetti et al*. [2007] for a comprehensive analysis of error sources affecting XBT data accuracy), which produce an accuracy of ±0.15°C [e.g., *Wright and Szabados*, 1989] in comparison to ±0.001°C for conductivity-temperature-depth (CTD) stations or ±0.005°C for Argo profiling floats. XBT data are increasingly being used in climate research, in which much greater measurement accuracy is required. This work examines the potential errors associated with estimates of integral quantities such as the Atlantic meridional overturning circulation (MOC) and meridional heat transport (MHT), given what is currently known about XBT uncertainty.

XBT biases are known to have impacted estimates of the interannual variability in ocean heat content and steric sea level, and corrections for the long-term influence of XBT biases on these estimates are the core of several studies [e.g., *Gouretski and Koltermann*, 2007; *Domingues et al*., 2008; *Levitus et al*., 2009].

Hanawa et al. [1995] first suggested a correction for XBT FRE biases; however, they recommended that correction not be implemented in the historical/real-time archive until proper meta data could be included to identify which fall rate was being used. Subsequent studies have shown that these biases are highly variable over time, mostly due to probe manufacturing changes [e.g., *Wijffels et al*., 2008; *DiNezio and Goni*, 2011]. Recently, a comparison of 4000 collocated CTD-XBT profiles provided a quantification of the uncertainty of annual historical biases in the XBT measurements taken since 1970 [*Cowley et al*., 2013].

Although a quantification of the impact of the XBT biases on the ocean heat content and sea level has been widely investigated, no estimates of the impact of XBT biases on the MOC and MHT have been reported. Given the great importance of the AX18 data for the current knowledge of the variability of the MOC and MHT in the South Atlantic [e.g., *Dong et al*., 2009, 2011; *Garzoli et al*., 2013], it is important to estimate all potential sources of uncertainty for evaluating current estimates and potentially improving future estimates. Previous studies analyzed other uncertainties of the XBT observational system to estimate the MOC and MHT at 34°S [e.g., *Baringer and Garzoli*, 2007; *Goes et al*., 2015], such as inferences about salinity, deep hydrography (below 800 m), temporal and spatial sampling, and reference level. The goal of this paper is to estimate the impact of the manufacturer's tolerances and historical changes of depth and temperature XBT biases on the MOC and MHT at 34°S. For this, we perform an uncertainty analysis on simulated XBT measurements using an eddy-resolving model reanalysis. To address the main goal, we will first describe the high-resolution global assimilation model and the methodology applied to simulate the XBT measurement biases in the model (section 2). In section 3 we will assess how the XBT measurement biases given by the manufacturer and by historical estimates may affect the MOC and MHT. Finally, we will discuss the results and put them in an observational perspective (section 4).

2. Model and Methods

In the present study we use data from the HYbrid Coordinate Ocean Model (HYCOM)/Naval Coupled Ocean Data Assimilation (NCODA) assimilative product [*Chassignet et al*., 2009] to simulate XBT measurements along 34°S. This model includes a Mercator grid extending between 78°S and 47°N, with an average of 1/12° (~7 km) horizontal spacing and 32 vertical layers. Surface forcing is from the Navy Operational Global Atmospheric Prediction System and includes 3-hourly and 0.5° wind stress, wind speed, heat flux (using bulk formula), and precipitation. Assimilated data include satellite sea height anomaly, in situ sea surface temperature (SST), and available in situ vertical temperature and salinity profiles from XBTs, Argo floats, and moored buoys. For the purpose of this work, we extend the coverage of the model output (from 2009 to 2013 in 7 day averages) to span from 1970 to 2010, every 15 days, by randomly resampling in time whole sections of temperature and salinity data from the initial 4 year coverage to create a time series of 40 years of data. To construct a particular month of a certain year in the extended data, we consider only the original model data for that particular month. Therefore, the amplitude of variability from weekly to interannual remains in the resampled fields, yet the transport time series estimated from this "control" data will have steady statistical properties, such as zero mean and negligible autocorrelation at time scales other than seasonal by definition, which will facilitate the analysis of the residual signals.

We simulate the XBT measurements on the resampled fields along 34.25°S (Figure 1a) in the model. This is the latitude on which most South Atlantic MOC studies have been based, including those obtained from the XBT transect AX18, which runs from Capetown to Buenos Aires. In order to simulate the XBT measurements in the model, we assume that only the model temperature in the upper ocean (surface to 800 m) and at every longitudinal grid point is measured by the XBTs. The upper ocean salinity is given by the model's annual local T-S relationships, and the deep temperature and salinity are monthly climatology estimates from the model.

In order to estimate the errors induced by the XBT fall rate and temperature biases, simulated XBT measurements are extracted from the model and subject to biases, similar to *Goes et al*. [2013]: the XBT depth biases are approximated by a depth offset (Z_0) and depth linear bias (Z_1) and thermal bias is approximated by a temperature offset (T_0). In an XBT system designed to monitor the integrated volume and heat transport across a section, XBT biases can contribute to MOC and MHT biases by changing the depth of the profile, and the geostrophic velocity reconstructed from temperature and salinity profiles, since salinity is also impacted because it is generally estimated from historical *T-S* relationships. Temperature changes due to biases will further affect the MHT because they enter directly into the integral of heat transport.

The reconstructed MOC strength and MHT have two independent dynamic terms, geostrophic and Ekman [*Goes et al*., 2015]. For the geostrophic component of the MOC and MHT, the velocities across the 34°S section are estimated by the thermal wind relationship, where the vertical shear is proportional to density gradients derived using salinity and temperature profiles along the section. Geostrophic velocities are calculated using a level of reference at the isopycnal depth of $\sigma_2 = 34.09$ kg m^{-3}, which is approximately

10.1002/2014GL061802

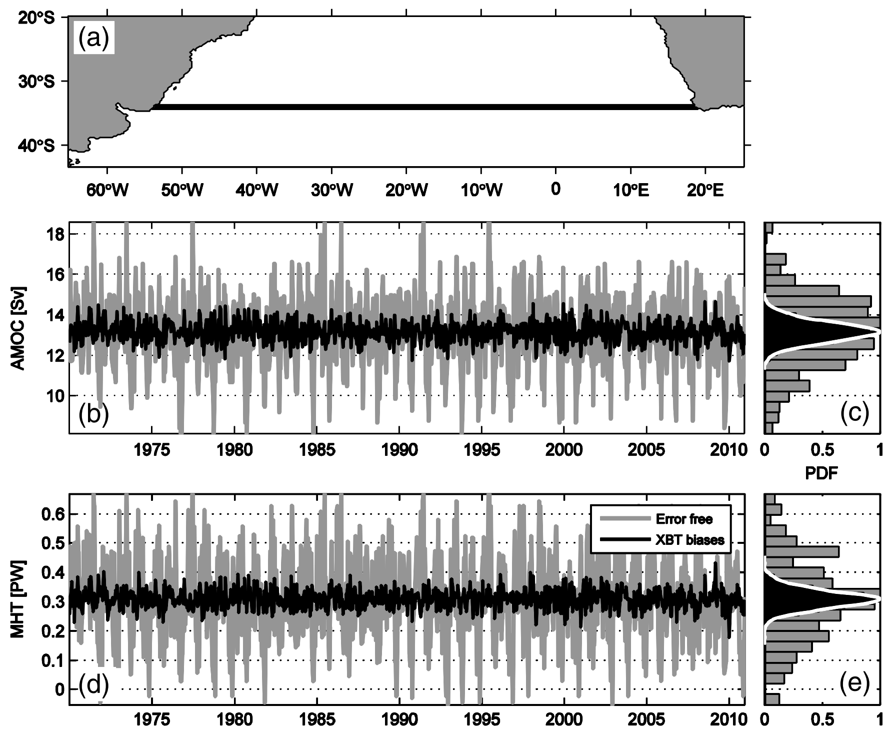

Figure 1. (a) Map containing the mean location of the AX18 XBT transect in the model. (b, d) Time series of the model MOC (Sv) and MHT (PW) (gray line) and respective MOC and MHT anomalies generated by random XBT errors (Z_0, Z_1, and T_0) approximated by a uniform distribution bounded by the manufacturer's tolerance errors. For scaling purposes, the mean values of the MOC and MHT are added to the anomaly time series. (c, e) Normalized histograms of the respective variability associated with the MOC and MHT time series (gray bars) and of the simulated errors (black area).

3500 m deep, or the bottom of the ocean, whichever is shallower. To account for the barotropic velocities the model climatological velocities are assumed at the location of the reference level. The Ekman component is calculated using the zonal wind stress of the model, assuming a constant Ekman layer depth of ~50 m. Note that XBT errors can impact both the geostrophic and Ekman components. As we assume a constant Ekman layer depth, XBT errors play no role in the Ekman component of the MOC. However, XBT pure temperature errors (T_0) may influence the MHT since temperature is included directly in the MHT calculations. According to our estimates, MHT errors associated with the Ekman component are minor (±0.0003 PW), and therefore, the Ekman response will be subtracted from the reconstructions; hence, only the geostrophic component will be further considered throughout this study.

3. Results

3.1. Manufacturer's Tolerance of XBT Biases and Their Impact on the MOC and MHT Variability

To assess the potential impact of the XBT measurement errors on weekly to interannual estimates, a comparison is performed on the magnitude of the generated MOC and MHT errors with respect to the natural variability of these quantities. To accomplish this, we generate the XBT error parameters drawn from uniform distributions bounded by the manufacturer's tolerance for the measurement error values [*Wright and Szabados*, 1989]. Thus, the measurement errors are randomly generated using the following range for the parameter settings: $Z_0 = \pm 5$ m, $Z_1 = \pm 2\%$ of depth, and $T_0 = \pm\ 0.15°C$. These three random errors are applied simultaneously to each of the profiles of the simulated XBT transect. Furthermore, we compare the distributions of the residuals of the inferred quantities (ΔMOC and ΔMHT, respectively) to the original variability of the MOC and MHT in the model (Figure 1).

The calculated geostrophic components of the MOC and MHT in the model are highly variable over time and have strong high-frequency components. The mean and standard deviation of the geostrophic MOC and MHT are 13.1 ± 1.8 Sv (1Sv = 10^6 m^3 s^{-1}) and 0.31 ± 0.14 PW (1 PW = 10^{15} W), respectively.

These values are slightly underestimated, partly because of the short 4 years underlying the reconstructed time series, but are not statistically different than the observed values along 34°S derived from the observed in situ XBT data along the AX18 transect (15.7 ± 2.6 Sv and 0.4 ± 0.17 PW) [*Dong et al*., 2011]. When all manufacturer XBT accuracy estimates are applied, the standard deviation of the ΔMOC is ±0.50 Sv, i.e., 3.8% of the mean geostrophic component MOC in the model, and for ΔMHT the standard deviation is ±0.03 PW, 9.7% of the geostrophic component MHT in the model. Therefore, although the errors are small in comparison to the mean MOC, the impact on the MHT across the section is more important. In addition, the 95% variability of the ΔMOC and ΔMHT errors can reach up to 1.1 Sv and 0.07 PW, which for a single section can represent up to 8% of the mean MOC and 22% of the mean MHT.

In a further analysis of the response of the MHT to the manufacturer's XBT errors, we divide the reconstructed MHT into its gyre and overturning components [*Bryan*, 1982; *Bryden and Imawaki*, 2001], where the overturning component is associated with zonal average (across gyre) transports, and the gyre component is defined as the deviation from the zonal average transports. Most of the total reconstructed MHT time series (Figure S1 in the supporting information) is driven by the overturning contribution, with a correlation of 93% and an average of 0.56 ± 0.24 PW. The gyre contribution is negative (southward) of −0.17 ± 0.09 PW, in agreement with previous results from observational studies [e.g., *Dong et al*., 2009]. The MHT errors associated with the XBT manufacturer's tolerance are about two times larger from the overturning contribution (± 0.027 PW) than from the gyre contribution (± 0.012 PW), although in percentage terms the error due to the gyre component (6.9%) is higher than the overturning component (4.6%).

3.2. Relationship Between Historical XBT Bias Parameters and the MOC/MHT Errors

To assess how the historical range of XBT measurement errors impact the MOC and MHT, we parameterize each historical XBT error, i.e., the depth offset (Z_0), depth linear bias (Z_1), and temperature offset (T_0), by randomly sampling a normal distribution $N(\mu, \sigma_\mu^2)$, where the respective mean (μ) and standard deviation (σ_μ) are given by the annual means and standard errors estimated in *Cowley et al*. [2013].

The time series of the three error parameters from years 1970 to 2010 are shown in Figures 2a–2c. When the three errors are combined along the 34°S section, the residuals of the MOC and MHT (Figures 2d and 2h, respectively) associated with these errors produce a long-term positive trend. This trend appears to increase in more recent years. The slope associated with this trend has increased since 1997, to 0.3 Sv decade^{-1} and 0.02 PW decade^{-1}, calculated using the cumulative sum method [*Page*, 1954; *Breaker*, 2007] for regime shift, local trend detection, and improvement of the signal/noise ratio.

The MOC and MHT response to the XBT measurement errors are very similar, and they show a correlation of 0.91 and a linear relationship of ΔMHT = 0.057 × ΔMOC (Figure 2l), whose slope is very close to the value 0.055 ± 0.003 PW reported by *Dong et al*. [2009]. This result, along with additional tests which neglect one of the errors in the MHT calculation, indicate that the error in velocity account for 91% of the variance of the MHT residuals, whereas the direct temperature error account for only approximately 9% of the MHT error due to XBT measurement.

When the XBT errors are applied separately, different relationships arise between the MOC responses to the historical range of the error parameter values (Figures 2i–2k). However, the MOC (and, therefore, the MHT) response over time is positively correlated to the values of each of the three error parameters, since all slopes are positive. Figures 2i–2k are displayed with the same range of ΔMOC in the vertical axis, while the horizontal axis is scaled to the observed range of the XBT error parameters. Hence, the relative differences of these slopes show that the effect of the FRE error (Figure 2i) is dominant over the other two error parameters, followed in order by depth offset and temperature offset errors.

3.3. Historical XBT Biases and the Detection of Trends in MOC and MHT

In the previous section we investigated the effect of the historical XBT errors on the variability of the MOC and MHT. The joint effect of the three simulated XBT error parameters is to produce a long-term positive trend in the considered quantities. Here we compare the multidecadal trends produced by XBT errors with the ones intrinsic from the MOC and MHT using our best knowledge, and analyze how XBT errors may impact the potential detection of MOC and MHT trends from 1970 to 2010 at 34°S.

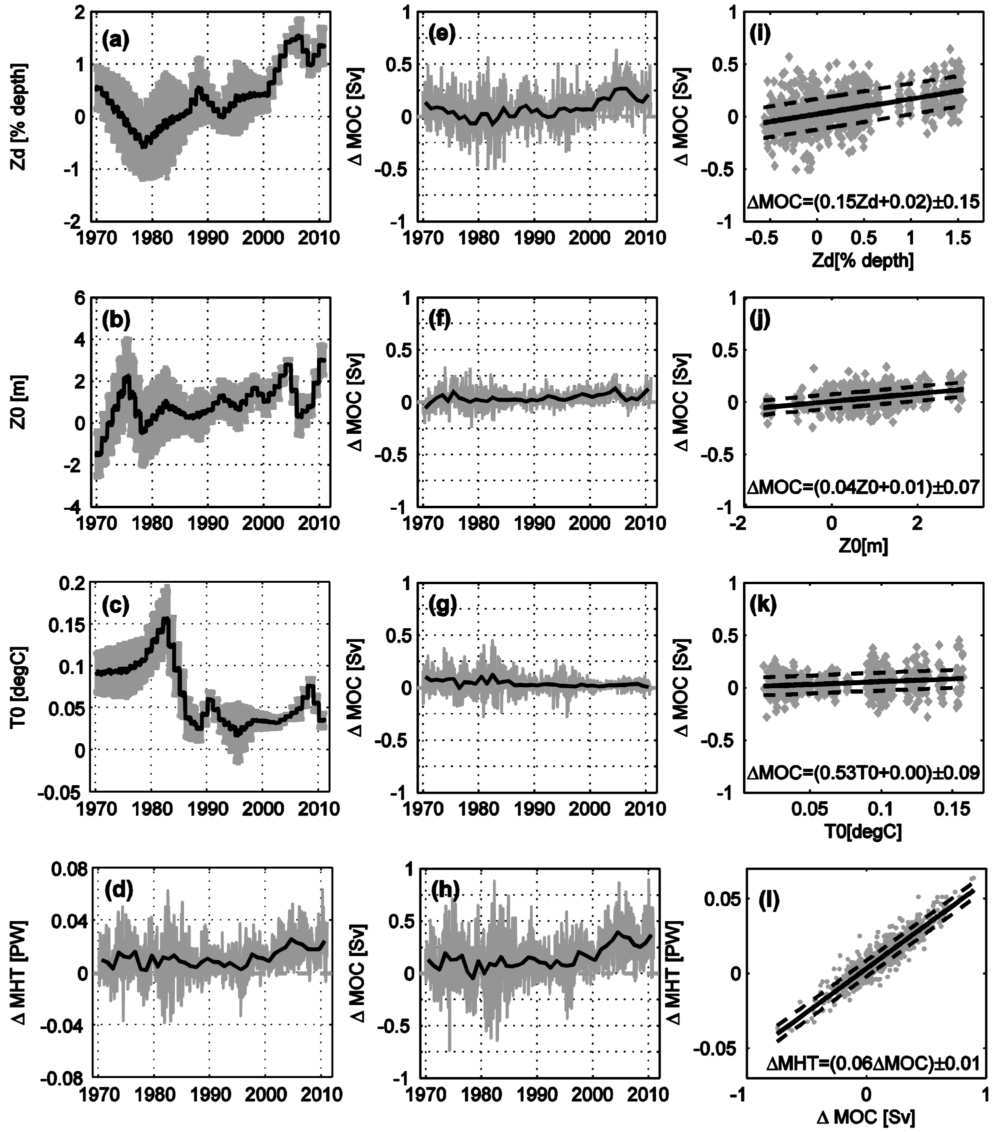

Figure 2. Time series of historical XBT biases estimated by *Cowley et al.* [2013] for the parameter (a) linear depth bias (Z_1), (b) depth offset (Z_0), and (c) temperature offset (T_0). The time series of MOC anomalies (ΔMOC) in response to the XBT historical biases are displayed in (e) for Z_1, (f) for Z_0, and (g) for T_0, and the relationship between ΔMOC and (i) Z_1, (j) Z_0, and (k) T_0 is shown. Also shown are the induced (d) ΔMHT and (h) ΔMOC for all errors combined and (l)the relationship between ΔMHT and ΔMOC.

Since there are no long-term direct observations that allow the estimation of linear trends in the geostrophic MOC and MHT components over this time period, we estimate these trends from an ocean reanalysis. For this, we use monthly outputs from Simple Ocean Data Assimilation version 2.1.6 (SODA) [*Carton and Giese*, 2008] for the period of 1970 to 2009. SODA applies a similar scheme to the one described in *Carton and Giese* [2008], with the differences that it uses ERA-Interim wind stress forcing instead of ERA-40 during 2002 to 2008, and assimilates all in situ oceanographic data with the *Levitus et al.* [2009] correction for XBT FRE error. The historical linear trends estimated in SODA since 1970 are positive (Figure 3); for the MOC the trend is 0.1 Sv decade^{-1}, and for MHT it is 0.006 PW decade^{-1}. We then add the estimated linear trends from SODA to the control time series of MOC and MHT from HYCOM/NCODA and compare the mean and uncertainty of the MOC and MHT residuals after 2000 relative to the control run to the decadal distributions of residuals caused by the three XBT errors. The mean and its respective standard error of MOC and MHT residuals relative to the control run are calculated using a bootstrap method with 300 samples, which is sufficient to allow

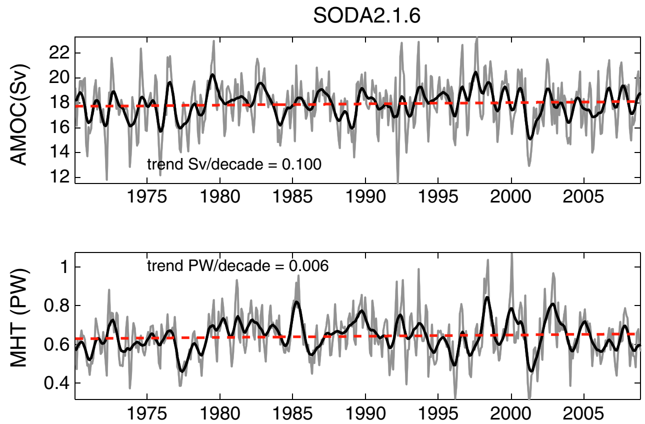

Figure 3. Time series of the (a) MOC and (b) MHT calculated from 1970 to 2009 in SODA. A 9 month running average is shown in black. The linear fits of the time series are displayed as dashed red lines. The estimated long-term trends from 1970 to 2009 are shown in each panel.

convergence of the estimates. The histograms of the bootstrapped distributions are shown in Figure 4. The variability of the MOC and MHT over their mean in the control simulation (solid black lines) are centered around zero by definition, and their estimated 95% confidence interval (CI = 1.96x standard error) [*Johnson*, 2001] is ±0.1 Sv for MOC and ±0.09 PW for MHT. When the calculated historical trends from SODA are added to the control simulation (dashed black line), the mean residual changes after the 2000s relative to the control and their 95% CI limits are 0.17 ± 0.19 Sv and 0.013 ± 0.020 PW. These high CI values relative to the mean suggest that there is high uncertainty associated with the detection of historical changes in the MOC and MHT. Therefore, the mean residuals of the trended time series after 2000 are not significantly different at the 95% CI, since these limits overlap with the ones from the control time series, as observed by the overlaps in their histograms.

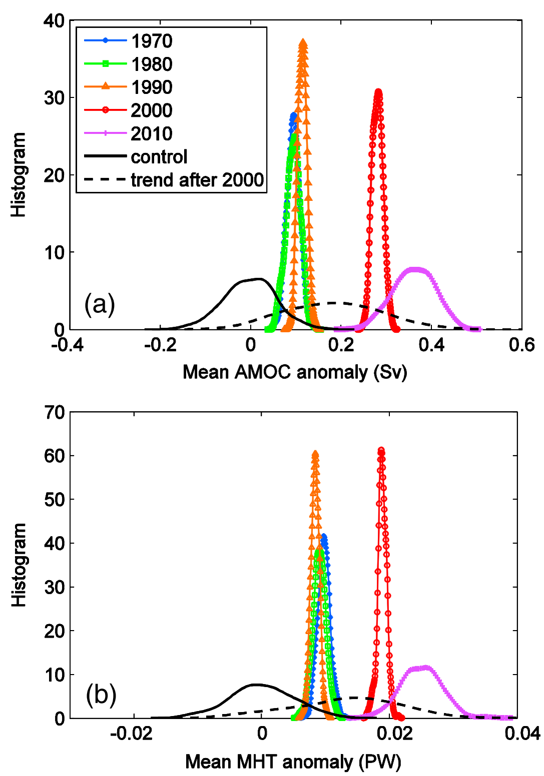

Figure 4. Histograms of bootstrapped distributions of the decadal mean of the (a) MOC and (b) MHT anomalies with respect to the control run. The colors are the anomalies caused by XBT measurement errors for 1970 (blue), 1980 (green), 1990 (orange), 2000 (red), and 2010 (purple). The control run distribution (black solid) and the control plus SODA trend after 2000 (black dashed) are also displayed.

The distributions of the decadal means of the AMOC and MHT residuals due to historical observational biases show changes over time. During the 1970s through the 1990s there are small, not significant positive residuals relative to the control simulation, centered at approximately 0.10 ± 0.02 Sv and 0.010 ± 0.002 PW. The 2000s show increased MOC and MHT biases of 0.28 ± 0.02 Sv and 0.0190 ± 0.001 PW, significant at the 95% CI. In the 2010s, even higher biases are observed, also significantly different than the control, of 0.38 ± 0.1 Sv and 0.025 ± 0.001 PW, which represent 3% and 8% of the mean value of the MOC and MHT, respectively. Therefore, the recent XBT biases are able to produce statistically significant changes in the MOC and MHT, and with the same sign yet larger than the historical trends in the MOC and MHT.

4. Discussion and Conclusions

In this study we use a high-resolution ocean assimilation model product to investigate the impact of historical biases in XBT measurements on the reconstructions of the South Atlantic meridional overturning circulation (MOC) and heat transport (MHT) at 34°S. For this, we simulate XBT measurements in the model using a methodology similar to the one used with observational data. The MHT error estimates associated with XBT-derived observations have been detailed in *Baringer and Garzoli* [2007], and more recently in *Goes et al.* [2015]. Although both of these studies examined several errors associated with the XBT system, such as salinity observations, shallow profiles, and sampling issues, these studies neglected random instrument errors due to the XBT design itself. Here we show that the XBT measurement errors are smaller than or comparable to other errors from an XBT observational system.

Random variability associated with the reported manufacturer's uncertainty can reach up to 1 Sv and 0.07 PW, values that may represent about 9–22% of the signal from a single section. These errors impact only the geostrophic part of the MOC, and are negligible for the Ekman component of the MHT. It is important to note that, although these errors can represent up to 22% of the mean strength of the MHT, in comparison to the seasonal-to-interannual variability of the MOC/MHT, the random errors associated with XBT measurements do not significantly impact those time scales. Therefore, previous estimates of seasonal and year-to-year variability of the MOC and MHT are sufficiently accurate even without FRE corrections.

On average, historical errors associated with the XBT measurement biases after 2010 account for approximately 3% of the strength of the mean geostrophic component of the MOC, and a stronger impact of ~8% of the mean MHT in the model. These values are similar to the mean standard deviations simulated using the manufacturer's tolerance values (4% and 9.7%, respectively). The MHT, whose computation is nonlinear and involves both circulation and temperature, is mostly affected (91%) by derived errors in circulation. The linear depth bias, which is caused by parameter uncertainty in the fall rate equation (FRE) of an XBT probe, accounts for most of the error in the MOC and MHT, followed by the depth offset due to differences in the entry velocity and the time response of the thermistor. The temperature offset, which is due to poorly calibrated thermistors during manufacturing and differences in recording systems, is the least significant source of errors in these calculations.

When compared to estimated historical changes of the MOC and MHT in an ocean reanalysis, which are slightly positive and not statistically significant, the recent changes (after 2000) associated with the XBT measurement biases have a slightly higher magnitude and are statistically significant at the 95% confidence level. The trend associated with the XBT measurement system, which increases after the late 1990s, is 0.3 Sv decade^{-1} and 0.02 PW decade^{-1}. This is concomitant to the time Sippican's XBT production factories moved from the USA to Mexico [*Wijffels et al*., 2008].

This study shows that FRE and temperature errors can potentially impact the detection of trends in the MOC and MHT at 34°S using XBT transect data and points to the critical importance of a continuous quantification of temporal changes in the mean XBT biases to allow correcting these systematic measurement errors in XBTs and to improve the accuracy of estimates of long-term changes of the MOC/MHT. This study adds value to the already established impact of correcting XBT biases on other climate indices, such as the historical global ocean heat content estimates [*Levitus et al*., 2009] and steric sea level changes [*Wijffels et al*., 2008]. Although the time series derived from this and the other high-density XBT transects are still very recent and too short (~10 to 15 years) to provide estimates of climate variability at decadal time scales, this study along with other recent studies provides insights into how to reduce the uncertainty inherent from monitoring systems based on XBT data.

Acknowledgments
Hycom/NCODA and SODA 2.1.6 model reanalysis data were obtained from www.hycom.org and http://coastwatch.pfeg.noaa.gov/erddap websites, respectively. Historical XBT bias parameters were obtained from http://www.nodc.noaa.gov/OC5/XBT_BIAS/cowley.html. This research was accomplished under the auspices of the Cooperative Institute for Marine and Atmospheric Studies (CIMAS), a cooperative institute of the University of Miami and the National Oceanic and Atmospheric Administration, cooperative agreement #NA17RJ1226, and was partly funded by the NOAA Climate Program Office and the NOAA Atlantic Oceanographic and Meteorological Laboratory (AOML).

The Editor thanks Rebecca Crowley and an anonymous reviewer for their assistance in evaluating this paper.

References

Baringer, M., and S. Garzoli (2007), Meridional heat transport determined with expendable bathythermographs. Part I: Error estimates from model and hydrographic data, *Deep Sea Res., Part I*, *54*(8), 1390–1401.

Breaker, L. C. (2007), A closer look at regime shifts based on coastal observations along the eastern boundary of the North Pacific, *Cont. Shelf Res.*, *27*, 2250–2277.

Bryan, K. (1982), Seasonal variation in meridional overturning and poleward heat transport in the Atlantic and Pacific Oceans: A model study, *J. Mar. Res.*, *40*, 39–53.

Bryden, H. L., and S. Imawaki (2001), Ocean heat transport, in *Ocean Circulation and Climate: Observing and Modelling the Global Ocean*, vol. 103, edited by G. Sidler, J. Church, and J. Gould, pp. 454–474, Academic Press.

Carton, J. A., and B. Giese (2008), A reanalysis of ocean climate using Simple Ocean Data Assimilation (SODA), *Mon. Weather Rev.*, *136*, 2999–3017.

Chassignet, E., et al. (2009), U.S. GODAE: Global ocean prediction with the HYbrid Coordinate Ocean Model (HYCOM), *Oceanography*, *22*(2), 64–75.

Cowley, R., S. Wijffels, L. Cheng, T. Boyer, and S. Kizu (2013), Biases in expendable bathythermograph data: A new view based on historical side-by-side comparisons, *J. Atmos. Oceanic Technol.*, *30*(6), 1195–1225.

DiNezio, P. N., and G. J. Goni (2011), Direct evidence of a changing fall-rate bias in XBTs manufactured during 1986–2008, *J. Atmos. Oceanic Technol.*, *28*, 1569–1578.

Domingues, C. M., J. A. Church, N. J. White, P. J. Gleckler, S. E. Wijffels, P. M. Barker, and J. R. Dunn (2008), Improved estimates of upper-ocean warming and multi-decadal sea-level rise, *Nature*, *453*, 1090–1093.

Dong, S., S. L. Garzoli, M. O. Baringer, C. S. Meinen, and G. J. Goni (2009), Interannual variations in the Atlantic Meridional Overturning Circulation and its relationship with the net northward heat transport in the South Atlantic, *Geophys. Res., Lett.*, *36*, L20606, doi:10.1029/2009GL039356.

Dong, S., M. Baringer, G. Goni, and S. Garzoli (2011), Importance of the assimilation of Argo float measurements on the Meridional Overturning Circulation in the South Atlantic, *Geophys. Res. Lett.*, *38*, L18603, doi:10.1029/2011GL048982.

Garzoli, S., M. O. Baringer, S. Dong, R. Perez, and Q. Yao (2013), South Atlantic meridional fluxes, *Deep Sea Res., Part I*, *71*, 21–32, doi:10.1016/j.dsr.2012.09.003.

Goes, M., G. Goni, and K. Keller (2013), Reducing biases in XBT measurements by including discrete information from pressure switches, *J. Atmos. Oceanic Technol.*, *30*, 810–824.

Goes, M., G. Goni, and S. Dong (2015), An optimal XBT-based monitoring system for the South Atlantic Meridional Overturning Circulation at 34°S, *J. Geophys. Res. Oceans*, *120*, doi:10.1002/2014JC010202.

Gouretski, V., and K. P. Koltermann (2007), How much is the ocean really warming?, *Geophys. Res. Lett.*, *34*, L01610, doi:10.1029/2006GL027834.

Hanawa, K., P. Raul, R. Bailey, A. Sy, and M. Szabados (1995), A new depth-time equation for Sippican or TSK T-7, T-6 and T-4 expendable bathythermographs (XBT), *Deep Sea Res., Part I*, *42*, 1423–1451.

Johnson, R. W. (2001), An introduction to the Bootstrap, *Teaching Stat.*, *23*(2), 49–54.

Levitus, S., J. I. Antonov, T. P. Boyer, R. A. Locarnini, H. E. Garcia, and A. V. Mishonov (2009), Global ocean heat content 1955–2008 in light of recently revealed instrumentation problems, *Geophys. Res. Lett.*, *36*, L07608, doi:10.1029/2008GL037155.

Page, E. S. (1954), Continuous inspection schemes, *Biometrika*, *41*, 100–115.

Reseghetti, F., M. Borghini, and G. M. R. Manzella (2007), Factors affecting the quality of XBT data—Results of analyses on profiles from the Western Mediterranean Sea, *Ocean Sci.*, *3*, 59–75, doi:10.5194/os-3-59-2007.

Wijffels, S. E., J. Willis, C. M. Domingues, P. Barker, N. J. White, A. Gronell, K. Ridgway, and J. A. Church (2008), Changing expendable bathythermograph fall rates and their impact on estimates of thermosteric sea level rise, *J. Clim.*, *21*, 5657.

Wright, D., and M. Szabados (1989), Field evaluation of real-time XBT systems, *Oceans*, *89*(5), 1621–1626.